Supplement of Clim. Past, 21, 1465–1480, 2025
https://doi.org/10.5194/cp-21-1465-2025-supplement

Climate of the Past
Open Access

Supplement of

SCUBIDO: a Bayesian modelling approach to reconstruct palaeoclimate from multivariate lake sediment data

Laura Boyall et al.

Correspondence to: Laura Boyall (l.boyall@bangor.ac.uk)

Supplementary Information 1: notations and variables used in the approach

Supplementary Table 1: Definitions of variables and model parameters used in the Bayesian framework.

Symbol	Description
C_i	Climate variable at time point i
C^m, C^f	Modern and fossil climate variable vectors
XRF_{ij}	Clr-transformed μXRF-CS data at depth i and element j
t_i	Calibrated age (in cal years BP) of depth i
θ	Vector of regression parameters ($\beta_{0,}$ $\beta_{1,}$ $\beta_{2,}$ $\mu_{0,}$)
σ_c	Standard deviation of the climate random walk
μ_{ij}	Mean of the multivariate normal distribution for element j j at depth i
Σ	Covariance matrix of residuals from the regression
MVN	Multivariate normal distribution
M_i	Vector of mean values μ_{ij} across all elements for depth i
ω_i	Variance term in the continuous-time random walk, scaled by age spacing
$\beta_{0,}$ $\beta_{1,}$ and β_2	Regression coefficients for element j
MDP	Marginal Data Posterior (posterior distribution for each time slice)
$\Sigma^{-1} \sim Wishart(R, k+1)$	Prior on inverse covariance matrix
$\sigma_c \sim \mathrm{LN}(a, b)$	Log-normal prior on random walk standard deviation

Supplementary Information 2: mathematical details on the marginal data posterior fitting.

Marginal data posteriors

In order to fit the marginal data posteriors (MDPs) we use the θ which was calculated in the calibration stage and introduce the fossil XRF data (XRF^{f}). We use k MDPs of each time slice as a reference to the sum of each multivariate normal distribution for each of the 11 chemical elements (j)

$$MDP_{ik} | \, C_i \sim MVN(\mu_{MDP_i}, prec_{MDP_i})$$

This stage also requires the use of a climate grid which is 50 possible climate values which are placed on a 50 x 50 regular grid. For example, if we were estimating temperature anomalies, the grid may look like a 50-part sequence from -3 °C to +3 °C, or precipitation may look like -100 mm to +100 mm. By having the climate grid helps the model choose sensible climate scenarios.

The output of the final MDP calculation is a MDP for each layer of the fossil XRF data which can be used within the final reconstruction of climate through time.

In the walk-through example (Section 4.0 main text), the climate grid chosen for Diss Mere was -3 °C and +3 °C having a range of 6 °C in total which is sufficient to cover the variability in temperatures reconstructed in the Holocene for other studies (Osman et al., 2021).

Supplementary Information 3 Diss Mere's non-varved chronology

The full chronology and age model for the non-varved sediments is described and published in Boyall et al. (2024). This is based on a combination of tephra layers that link the non-varved and the varve chronology, radiocarbon dates and the 1963 CE ^{137}Cs peak. The average age uncertainty for the non-varved section of Diss Mere is ± 65 years and thus is higher than the varve chronology. During the calibration period (1700 – 1932 CE), the age uncertainty is smaller at the top of the sequence with a maximum uncertainty of ± 22 years between 1932 CE and 1800 CE, however this increases gradually to ± 110 years for the following century (Supplementary Figure 1). The sedimentation rate within this period is very high (0.15 cm/year) and includes up to 20 data points per year.

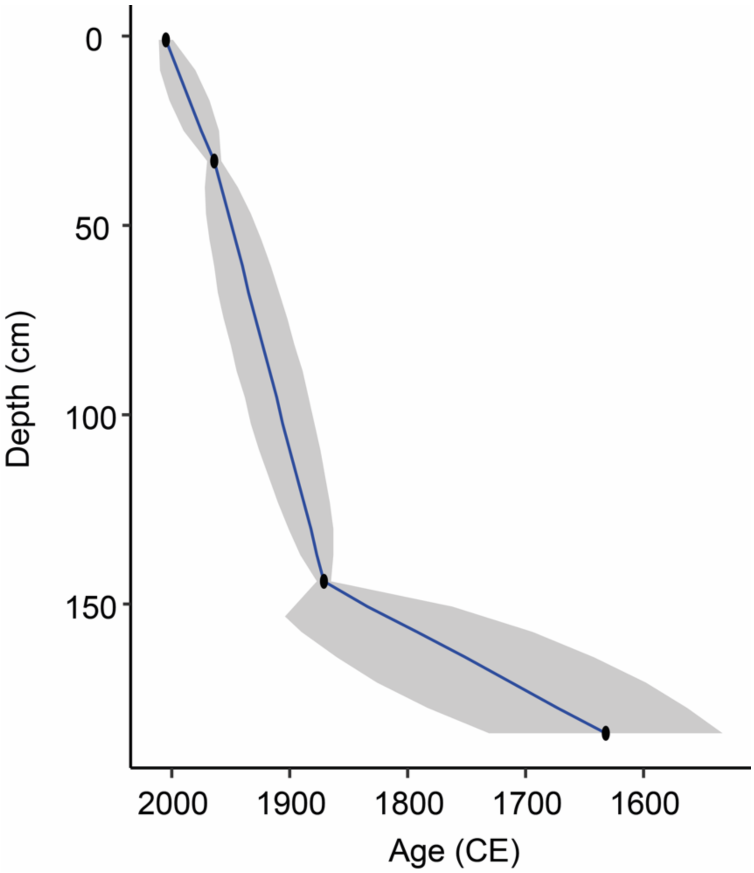

Supplementary Figure 1: Age-depth model for Diss Mere during the calibration period and the full age model for the non-varved section of the Diss Mere sediments can be found in Boyall et al. (2024).

Supplementary Information 4: locations of meteorological weather stations for Nautajärvi calibration

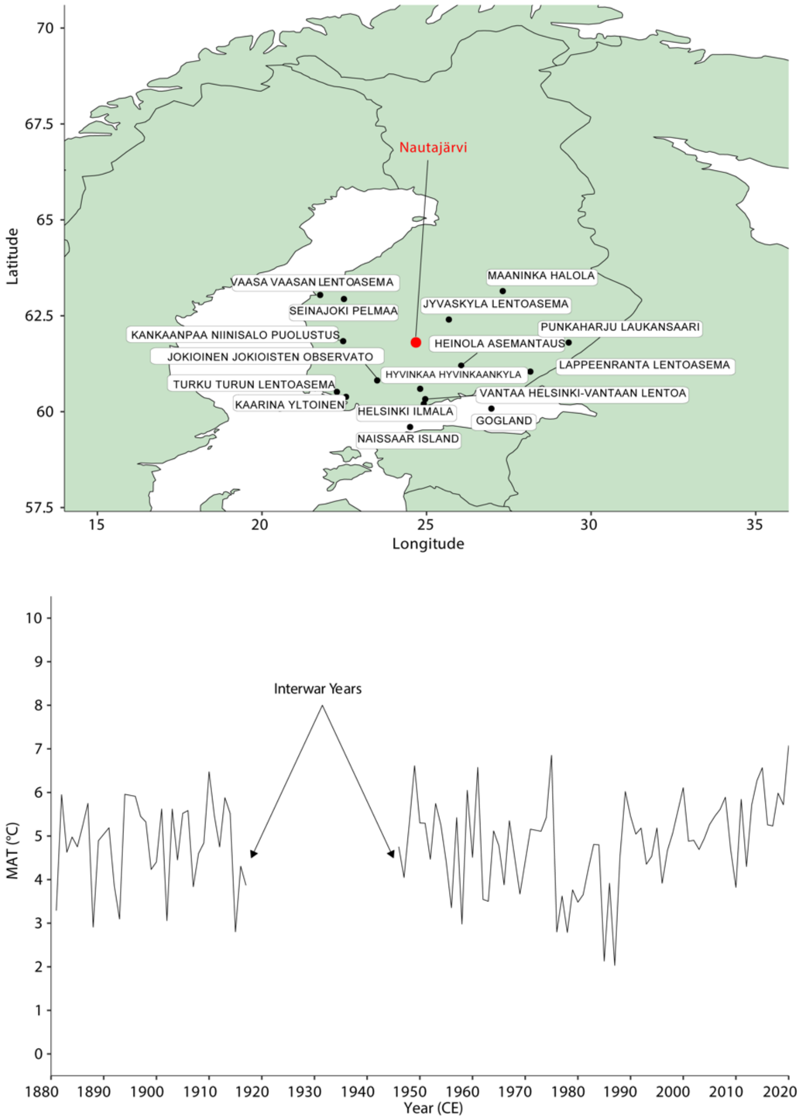

Supplementary Figure 2: A figure showing the locations of the weather stations used to build a composite record of annual mean temperatures for Nautajärvi and a timeseries showing the record with an interwar period of no data.

Supplementary Information 5: Validation results for Nautajärvi.

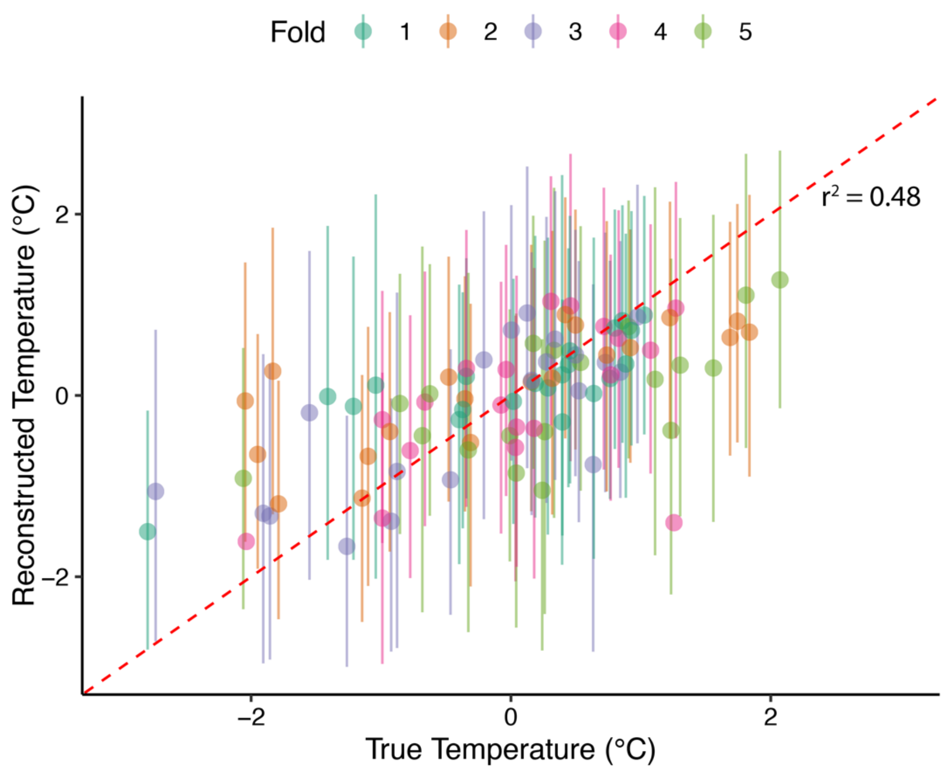

Supplementary Figure 3: True vs reconstructed temperature for Nautajärvi with the colours dots and bars representing the fold results for the median and confidence intervals, respectively.

The same out-of-sample validation approach detailed in the main manuscript for Diss Mere was applied on the calibration period for Nautajärvi. The coverage percentage for is 94.95% and the r^2 value is 0.48 (P = <0.001).

Supplementary Information 6: Absolute temperatures of the Diss Mere and Nautajärvi reconstruction

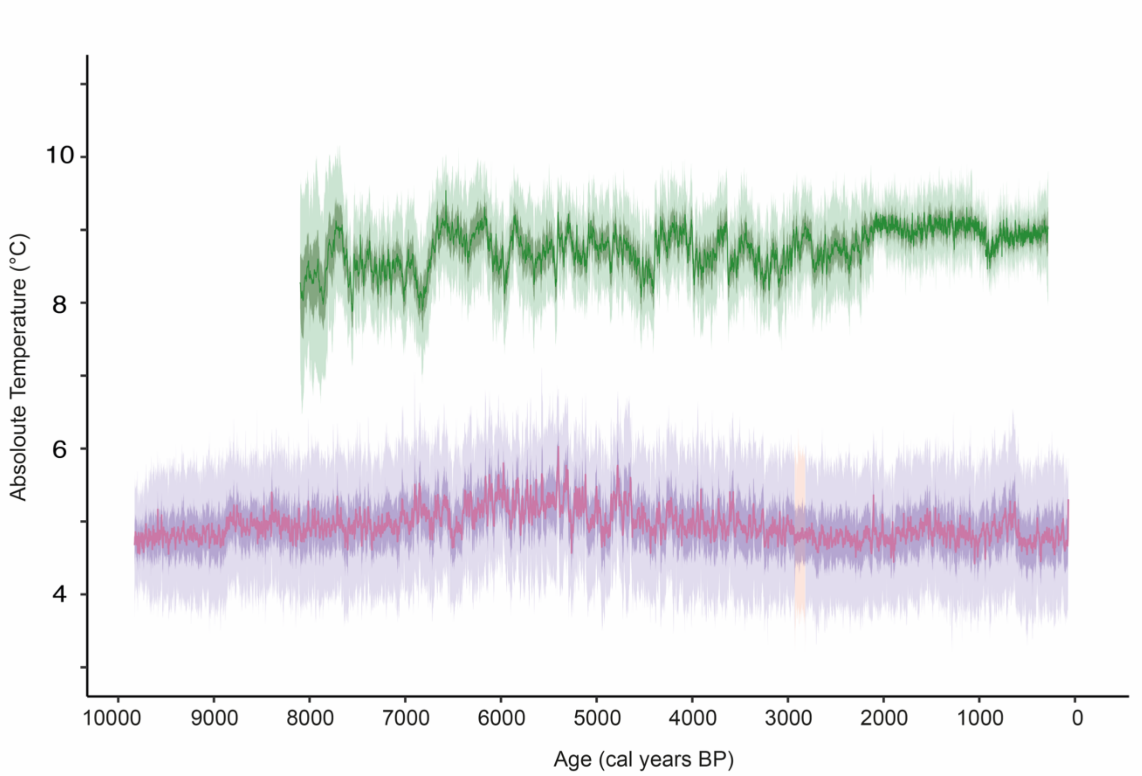

Supplementary Figure 4: A figure showing the Diss Mere (green) and Nautajärvi (purple) reconstructions in absolute temperatures

Supplementary Information 7: Diss Mere and Nautajärvi temperature reconstructions

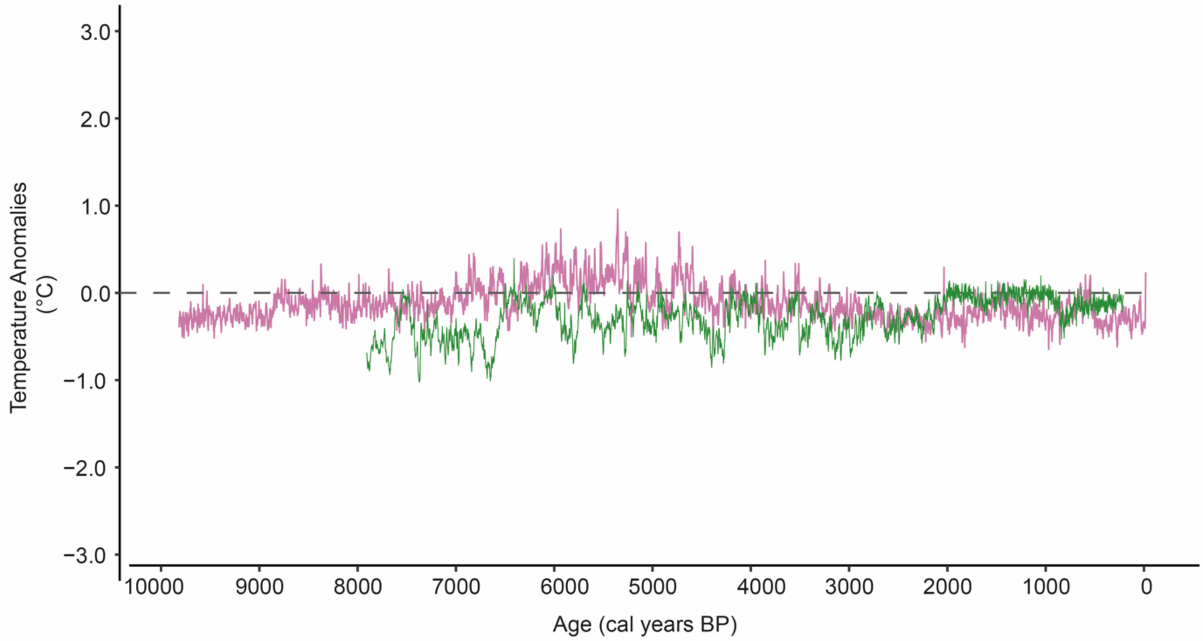

Supplementary Figure 5: Diss Mere (green) and Nautajärvi (purple) reconstructions without uncertainty envelopes. Reference period 1991-2020